

# Earthquake-Risk Mapping

DR. ERVIN Y. KEDAR<sup>\*</sup>  
WILLIAM PATERSON  
College of New Jersey  
Wayne, N.J. 07470  
DR. SHIN-YI HSU  
State University of New York  
Binghamton, New York 13901

Fault lineaments were located from space photographs and their seismic potential was recognized far in advance of the San Fernando Valley earthquake.

## INTRODUCTION

THE NEED FOR a large scale earthquake-risk (or seismic-risk) map has been felt for a long time. A seismic risk map of the United States was first prepared in 1948 by F. P. Ulrich of the Coast and Geodetic Survey.<sup>1</sup> It was revised and published in 1969, based on additional seismic studies.<sup>2</sup> The original and modified seismic-risk maps are based on the distribution of earthquake intensities in-

very small scale and very highly generalized; therefore, a much more detailed large scale map is needed for investigating earthquake hazards in the future.

The state of the art in seismology is such that it is yet impossible to predict earthquakes, i.e., when an earthquake might occur and at what magnitude. However, as earthquakes are the results of earth's crustal movements and adjustments, it is obvious that

---

*ABSTRACT: Earthquake risk mapping is a synoptic analysis of the likelihood of the occurrence of earthquakes in different locales. It is achieved by combining space photographic data, inferred structural lineaments, geological records of fault lines, and seismic history of the area. The test area of this study is the Greater Los Angeles vicinity occupying 100 × 100 square miles. A grid with inner cell size of 10 × 10 square miles was used as a control for constructing choropleth and isopleth maps of seismic risks. The pattern revealed by the three response variables differed slightly. The final map integrating statistically the three variables represents the risk nature of the area. It indicates that a low-risk zone is centered at the Los Angeles Basin. The risk increases in three directions: (1) to the northwest along San Gabriel Mountain, (2) to the southeast along Santa Ana Mountain, and (3) to the northeast towards San Bernardino Mountain. The risk map should be considered dynamic. The constant inflow of related data should be processed constantly by means of statistical methods and computer graphics.*

---

corporated with the known seismic history of the United States, the strain released and large-scale geologic features believed to be related to seismic activities.<sup>3</sup> The map is an isoplethic map, containing four probable frequency classes of damaging earthquakes: (1) Zone 0—no damage, (2) Zone 1—minor damage, (3) Zone 2—moderate damage, and (4) Zone 3—major damage.

This seismic-risk map is constructed on a

<sup>\*</sup> Presented at the Annual Convention of the American Society of Photogrammetry, Washington, D.C., March 1972.

geologic evidences on land surfaces can indicate to a certain degree where most of the large earthquakes will occur in the future.

Almost all earthquakes (more than 90 percent) are shallow and occur within the crustal layer of the earth. Earthquake risk mapping should include all of the measurable geomorphotectonic variables such as: strain accumulation, rate of rock creep, vertical and horizontal displacements, gravity measurements of the crust.

Above all, though, it has been proved that certain earth crustal phenomena may be bet-

ter understood from photographs taken in space rather than when studied on the surface of earth. Crustal displacements, plutonism, and rising and sinking of crustal areas are among those factors that can better be detected from space platforms. Conventional geotectonic, geologic, geomorphologic and geophysical methods are not sufficient for the studies of large regional units. If shear faults have displacements of hundreds of miles, an investigator cannot observe the geotectonic pattern as a whole. Therefore, investigators must use other approaches to solve the problem of how to comprehend the dimension of large structural phenomena. Space photography and remote sensors seem to be a partial answer to this problem.

Sections of the surface of the earth between latitudes of 35° N and 35° S are displayed in several series of photographs obtained from Gemini and Apollo Missions. Many of these high-quality color photographs may be viewed in stereopairs. These photographs can make a unique contribution to earthquake-risk mapping by generalizing photographically secondary and tertiary geomorphotectonic elements and the appearance of the first-rank structural features of the crust. In addition, a single photographic frame gives a synoptic view of an entire region. This photography removes the geologist from his close-to-earth viewpoint and provides him with a perspective view of the surface, a dimension never before seen in a conventional aerial photograph.

It was concluded for the San Fernando earthquake of February, 1971, that "... many

of the faults that broke during the earthquake were not generally shown in geologic maps published prior to the event, and none had been considered particularly active..."<sup>4</sup> However, the same fault lineaments were located from space photographs and their seismic potential was recognized far in advance of that earthquake.

#### CASE STUDY: TRANSVERSE RANGES, CALIFORNIA

Small-scale oblique Ektachrome photographs obtained from Apollo spacecraft have been studied to determine their usefulness in geomorphologic, tectonic processes, and earthquake-risk mapping in the coastal portion of Southern California.<sup>5</sup> Two sets of 70-mm stereoscopic pairs (NASA photographs AS7-11-2019/2020 and AS7-2021/2022) of the Transverse Ranges covered an area extending from the Pacific Ocean at Point Arguello on the west to the Mojave Desert on the east and from the southern end of the San Joaquin Valley on the north to the Los Angeles basin and the San Bernardino Mountains on the south (Figures 1 and 2).

The Transverse Range, which is considered to be highly *mismatched stratigraphically* and marked by complexity and controversy, was studied in detail.<sup>6</sup> The region is a transition zone between the San Andreas Fault southern system and the San Andreas Fault northern system. The space photographs have been studied in conjunction with the following conventional sources: the Los Angeles Sheet of the Geologic Map of California,<sup>7</sup> the Geologic Map of the Transverse Range

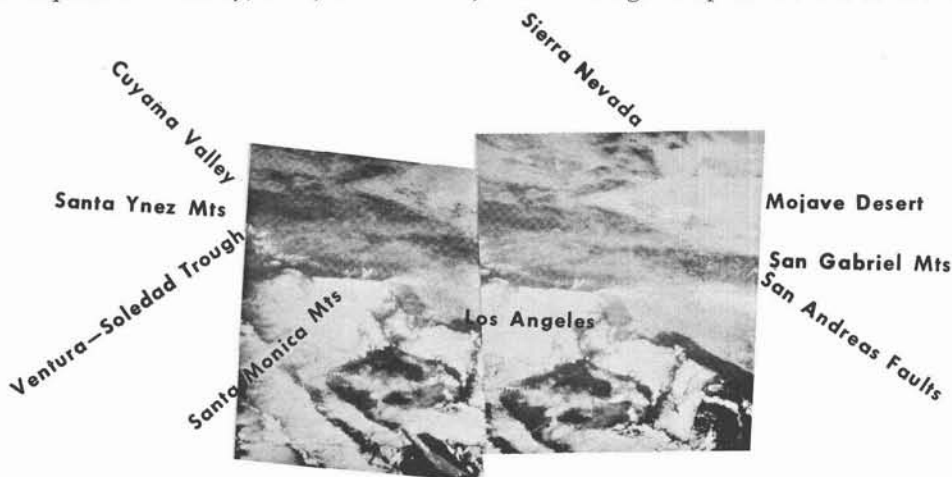


FIG. 1. 70-mm stereopair of the Los Angeles area taken from Apollo 7 spacecraft.

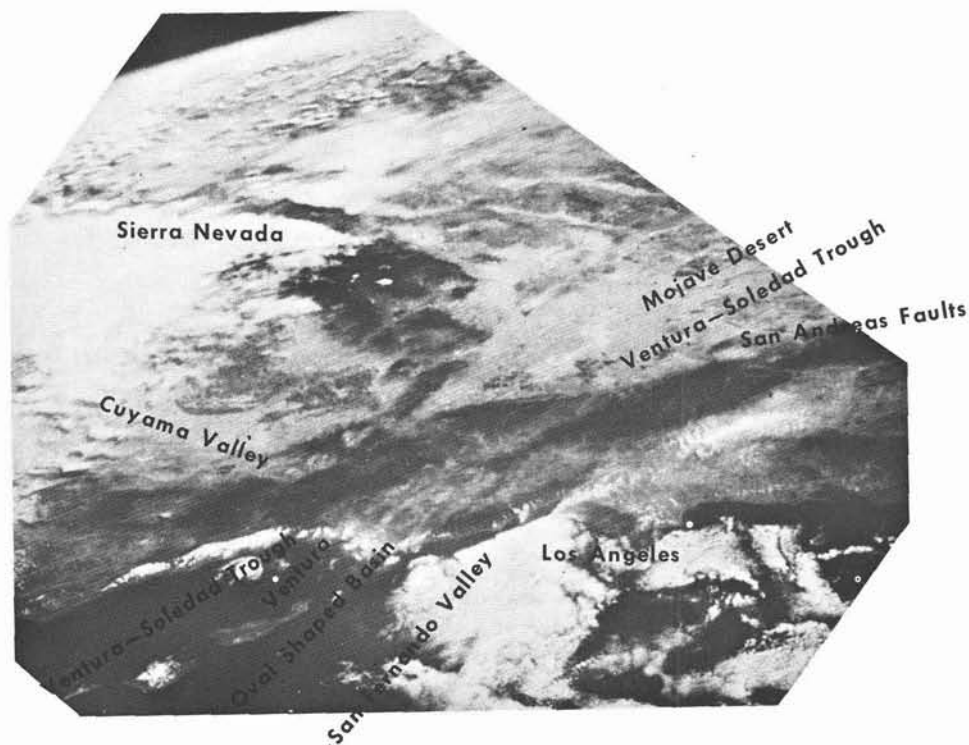


FIG. 2. Photograph of the Los Angeles area taken from Apollo 7 spacecraft.

Province,<sup>8</sup> and the Geology of the Central Santa Ynez Mountains, Santa Barbara County, California.<sup>9</sup> A comparison of the space photographs with conventional sources concerning geomorphotectonics was made as follows:

- Each conventional source fails to emphasize the main structural lineaments bounding the San Fernando Valley (Simi-Hills, Santa Monica Mountains, and Verdugo Mountains). These structural lineaments, which can be easily seen from space photographs, are apparently the major morphotectonic features in the tectonic framework of San Fernando Valley (See Figure 3).
- Each conventional source fails to show the oval-shaped sedimentary basin bounded by Oakridge, South Mountain and the Santa Susana Mountains on one side, and the volcanic ridge extending from Point Muzu toward the mountain knot in the higher Santa Susana Mountain complex on the other side.

The conventional sources fail to portray these facts and information because they are either over-generalized or under-generalized.

The Geologic Map of Transverse Range Province, Southern California,<sup>10</sup> shows only faultlines and rock-age distribution but lacks drainage patterns and contour lines. The Los

Angeles Geologic Map of California has too much information (road systems, railroad, power lines) and makes no distinction between major faults and local faults.

Space photography is the only generalized, yet selective, source of information; although it presents an oblique distorted view it is nevertheless a mandatory information source. The inferences from these figures suggest that definite order exists in the crustal displacement and deformation of at least a portion of the Transverse Range. It is widely accepted that acute tectonic mobility is associated with the Transverse Range and that the strike-slip displacement of its crustal block is a common geologic feature. However, the amount of lateral displacement in the older rocks of the Transverse Range (Figure 4) has not yet been substantiated by observing in the space photographs how closely the *arrowhead* shapes of the southeastern edges of the Sierra Madre Mountains and the Cuyama Valley match each other in size and configuration. The separation of the Eocene clastic rocks in the Big Pine Mountains and the location of the Mount Pinos granite intrusion in the gap also support the course of geomorphotectonic events suggested in this report.

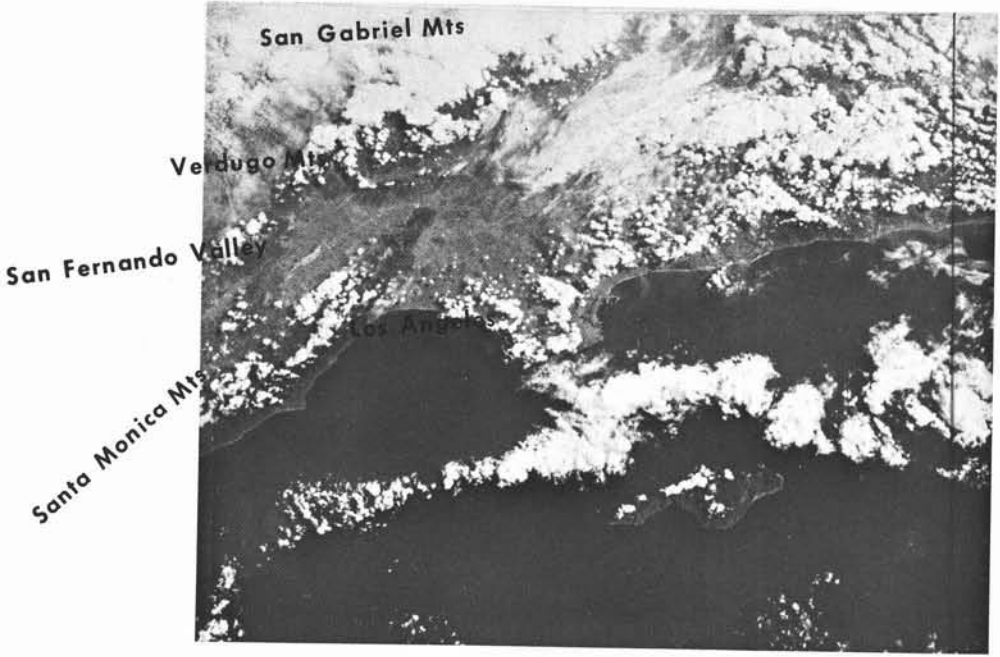
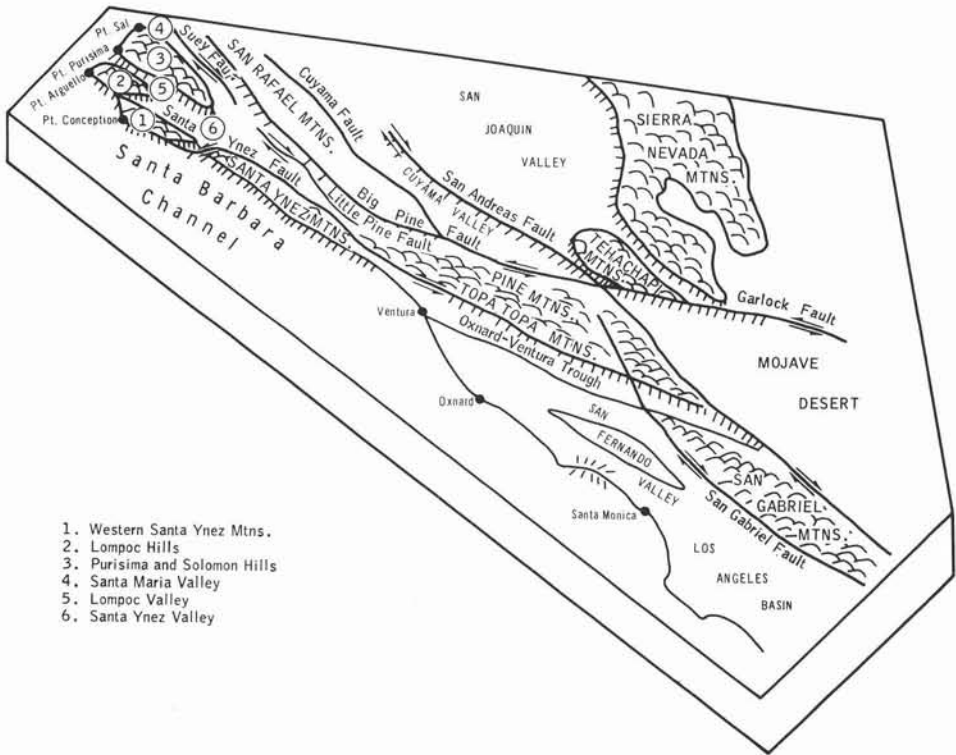


FIG. 3. Apollo 7 photograph of the Los Angeles area.



- 1. Western Santa Ynez Mtns.
- 2. Lompoc Hills
- 3. Purisima and Solomon Hills
- 4. Santa Maria Valley
- 5. Lompoc Valley
- 6. Santa Ynez Valley

FIG. 4. Reconstruction of the transverse ranges (after Apollo 7 photograph AS7-11-2020 shown in Figure 1).

A crustal basin along the Ventura-Soledad trough is readily visible on the photograph and appears to have originated with the northwestern displacement of the northern crustal complex. Whether this displacement occurred along the San Gabriel strike-slip fault or along the San Andreas Fault has not been established, although the San Gabriel strike-slip fault is suggested as the more likely location.<sup>15</sup>

#### EARTHQUAKE-RISK MAPPING

An earthquake-risk map is to show relative likelihood of the occurrence of earthquakes in different locales. It will be constructed according to certain measurable variables (related to earthquakes) obtained from space photos, geologic maps, and seismic records. These variables are:

- ★ Relative density of structural lines shown on space photos.
- ★ Relative density of faults (lines) shown on geologic maps.
- ★ Cumulative seismic scores obtained from frequency and magnitude of earthquakes.

The Greater Los Angeles area (Figure 5) is our study area. It occupies  $100 \times 100$  square miles. An inner-grid with cell size of  $10 \times 10$  square miles was used as a control for constructing choropleth and isopleth maps of earthquake risks. Each of the seismic-risk variables was mapped first and then combined into a final earthquake risk.

Both the space and geologic data are classified into six categories of risks as follows:

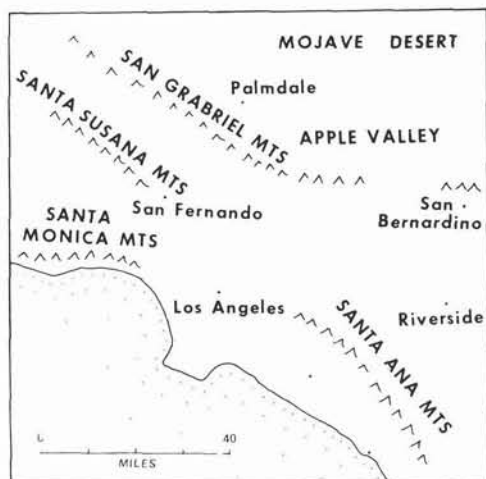
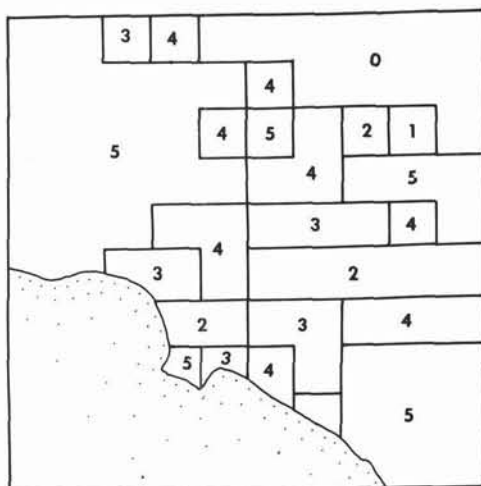


FIG. 5. Map of the greater Los Angeles study area.



0	None	3	High Potential
1	Low Potential	4	Higher Potential
2	Moderate Potential	5	Extremely High Potential

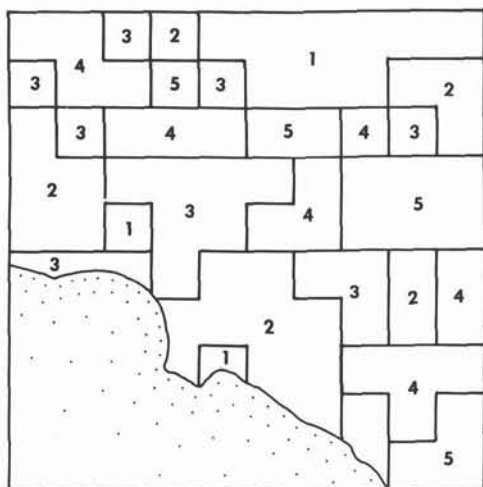
FIG. 6. Seismic potential from space data.

5	extremely high	potential-seismicity
4	higher	potential-seismicity
3	high	potential-seismicity
2	moderate	potential-seismicity
1	low	potential-seismicity
0	none	potential-seismicity

The pattern of seismic risks shown in Figure 6 constructed from space data is informative. The extremely high-risk areas inferred from space photographs are located in San Gabriel, Santa Susana, Santa Monica Mountains in the northwest corner and Santa Ana Mountains with Peris Basin in the southeast corner. A belt of moderate risk is located from Redlands to Los Angeles. The no-risk and low-risk areas are located in Mojave Desert and Apple Valley.

The risk pattern shown on Figure 7 is constructed from geologic data and is slightly different from the information collected from space photos. The degree of risk in Santa Susana and Santa Monica Mountains is reduced to high and moderate risks, and that in Santa Ana Mountains is also reduced to higher and high risks. On the other hand, Mojave Desert and Victory Valley are classified as low- and moderate-risk areas. The discrepancy between these two patterns is due to the advantages and disadvantages of space versus ground information concerning geological structural lines. This was discussed in previous sections.





0 None	3 High Potential
1 Low Potential	4 Higher Potential
2 Moderate Potential	5 Extremely High Potential

FIG. 7. Seismic potential from geologic data.

The third seismic-risk map was constructed from seismic history data concerning both frequency and magnitude of earthquakes.

The cumulative score is computed as follows:

$$\text{Risk Score} = \frac{\sum_{K=1}^n 10^{L_K}}{n}$$

where  $L$  is earthquake magnitude registered on Richter Scale and  $K$  is the frequency of earthquakes.

Figure 8 was constructed based upon four-year records: 1965-1968. It is, therefore, only a case study intended to show the method, rather than a map of actual seismic value. The risk pattern coincides generally with those on Figures 6 and 7. However, two highs located at San Bernardino and downtown Los Angeles are off ten miles.

The above-discussed three maps are constructed according to a single variable. To obtain a better map having classification value, all of the three variables have to be taken into consideration. There are several methods which can be used to combine them. The simplest of all is to take the average of the three values, provided that their unit values are the same. In addition, a more complicated statistical method, the principle component, is also applicable. The component scores of the cells are to be used to show

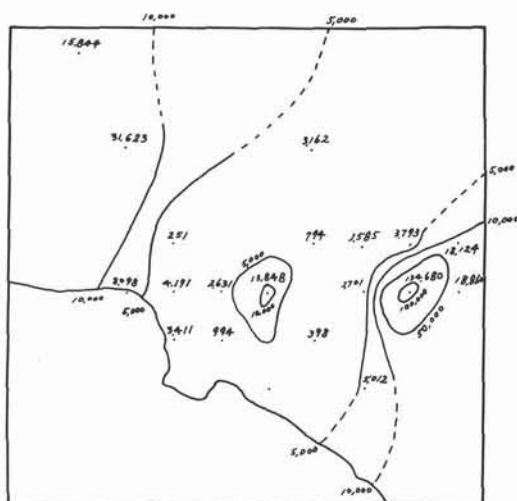


FIG. 8. Seismic potential from seismic data 1965-1968.

the relative value of risk. (Of course, we hope that the first component is sufficient.)

In our case study, we chose the simplest methods. First, the risk values obtained from space and geologic data are translated into risk scores comparable to those in Figure 6, as follows:

#### Risk Value

Risk Score = 10 (Ranging from 0 to 5).

Then the combined risk score is taken as the means of the three risk scores as follows:

Combined Risk Score = Average of (Risk score from space data + Risk score from geologic data + Risk score from seismic data).

A map (Figure 9) of combined risk score

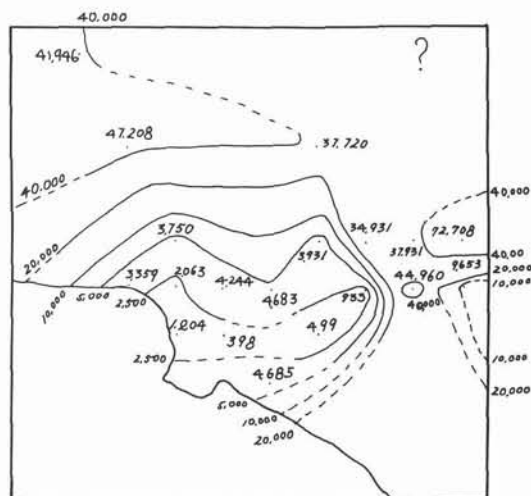


FIG. 9. Earthquake-risk map.

was constructed according to the control points having seismic data. The risk pattern shown on Figure 9 is similar to that of space data. The three *highs* are located in San Gabriel, Santa Ana, San Bernardino Mountains.

The *low* is located in Los Angeles Basin (Fullerton to downtown Los Angeles). The directions of risk increase are three:

1. From Los Angeles Basin to the northeast (San Gabriel Mountains),
2. From Los Angeles Basin to Santa Ana Mountains,
3. From Los Angeles to San Bernardino Mountains.

The risk score in Mojave Desert is unknown, owing to the lack of seismic data (for 1967-1968).

This combined earthquake-risk map should be viewed as a synoptic map similar to weather maps. The pattern of risk changes according to the inflow of earthquake and other related data. The response variables can also be increased. For instance, we can take into consideration the gravity anomaly data, the distances from the highest risk-score centers. Automatic analysis of earthquake risk can also be achieved by combining the mathematical models discussed and displaying them by computer graphics.

#### REFERENCES

1. Coffman, Jerry L., *United States Earthquakes 1968*, U.S. Dept. of Commerce, ESSA and C&GS, Washington, D.C. 1970, p. 8.
2. Seismology, Responsibility and Requirement of a Growing Science Part I: Summary and Recommendations, *Report of the Committee on Seismology*, Division of Earth Sciences, NRC/NAS, Washington, D.C., 1969, pp. 11-12.
3. A revised edition of *Earthquake History of the United States* has been published in 1971.
4. *The San Fernando Earthquake of February 9, 1971*, Lessons From a Moderate Earthquake on the Fringe of a Densely Populated Region, by NRC, NAC, Washington, D.C., 1971, p. 4.
5. Kedar, E. Y., Space Photographs of the Earth in the Study of Geotectonics, AAS69-579, Vol. 23, *Science and Earth Technology*, 1969. Also presented at the *American Astronautical Society National Meeting*, Paper no. AAS69-579, New Mexico State University, Las Cruces, New Mexico, October 23-25, 1969.
6. Crowell, J. C., *The California Coast Ranges. A Coast to Coast Tectonic Study of the United States: UMR J., No. 1*, V. H. McNutt-Geol. Dept. Colloquium Ser. I, 1968, pp. 133-156.
7. Los Angeles Sheet of the Geologic Map, 1955.
8. Geologic Map of the Transverse Range Province, Southern California, Department of Natural Resources, State of California, 1954.
9. *Geology of the Central Santa Ynez Mountains*, Santa Barbara County, California, 1966.
10. See Reference 8 above.
11. Dibblee, T. W., *Geology of the Central Santa Ynez Mountains*, Santa Barbara County, California, Calif. Div. Mines & Geol. Bull. 186, 1966.
12. Menard, H. W., Shear Zones of the Northeastern Pacific Ocean and Anomalous Structural Trends of Western North America. *Geol. Soc. Am. Bull.*, Vol. 64, No. 12, Pt. 2, Dec. 1953, p. 1512.
13. Hill, M. L., and Dibblee, T. W., Jr., San Andreas, Garlock, and Big Pine Faults, California—A Study of the Character, History, and Tectonic Significance of Their Displacements. *Geol. Soc. Am. Bull.*, Vol. 64, No. 4, Apr. 1953, pp. 443-458.
14. Kutina, J., Hydrothermal Ore Deposits in the Western United States: A New Concept of Structural Control Distribution. *Science*, Vol. 165; Sept. 12, 1969, pp. 1113-1119.
15. Kedar, E. Y., Transverse Range: Tectonic Inferences from Earth Photographs from Space, NASA/MSC, TF7-2, June 1970.